Spectroscopic properties of Ni^{2+} in $RbCaF_3$ and $RbCdF_3$

1993 J. Phys.: Condens. Matter 5 747

(http://iopscience.iop.org/0953-8984/5/6/011)

J. Phys.: Condens. Matter 5 (1993) 747–756. Printed in the UK

Spectroscopic properties of Ni^{2+} in $RbCaF_3$ and $RbCdF_3$

B Villacampa†, R Alcalá†, P J Alonso† and J M Spaeth‡

† Instituto de Ciencia de Materiales de Aragón, Universidad de Zaragoza—CSIC, Facultad de Ciencias, Plaza San Francisco s/n, 50009 Zaragoza, Spain
‡ Universität-GH Paderborn, Fachbereich Physik, Postfach 1621, D-4790 Paderborn, Federal Republic of Germany

Received 22 September 1992

Abstract. A new photoluminescence band corresponding to the $^1T_{2g}(D) \Rightarrow {}^3T_{1g}(F)$ electronic transition of Ni^{2+} ions has been obtained in nickel-doped $RbCaF_3$ and $RbCdF_3$. The structure of this band together with those of the other two previously reported emissions from the $^1T_{2g}(D)$ level to the $^3A_{2g}(F)$ and $^3T_{2g}(F)$ levels have been measured at 10 K and discussed in terms of spin–orbit and phonon interactions. The EPR spectrum of Ni^{2+} ions has also been measured in $RbCaF_3$ as a function of temperature. Above the cubic–tetragonal phase transition temperature ($T_c = 195$ K) a cubic signal is observed with an isotropic g-factor ($g = 2.36 \pm 0.01$). Below T_c the signal becomes tetragonal with $g_{\parallel} = 2.32 \pm 0.01$, $g_{\perp} = 2.30 \pm 0.01$ and $D = 25.3 \pm 0.5$ GHz at 80 K. The crystal field parameter D shows the temperature dependence $D(T) = D_0|T - T_c|^{0.48}$. From these results a value for the critical exponent of the transition $\beta = 0.24$ has been derived in good agreement with those obtained using other techniques.

1. Introduction

Although the spectroscopic properties of Ni^{2+} ions in fluoride crystals have been studied for many years [1–5] the search for new materials for tunable solid state lasers in the near infrared and the observation of laser action in Ni-doped MgF_2 and $KMgF_3$ [6, 7] has renewed interest in the spectroscopy of divalent Ni ions in fluorides [8–10].

Ni^{2+} is one of the few 3d ions that show luminescent emissions due to electronic transitions among excited states. A detailed study of these emissions including their low-temperature structures provides valuable information on the dynamics of excited states higher than the first as well as on their spin–orbit and phonon interactions.

Usually three emissions have been reported for Ni^{2+}, one of them corresponding to the $^3T_{2g}(F) \Rightarrow {}^3A_{2g}(F)$ transition from the first excited state to the ground state and the other two associated with the $^1T_{2g}(D) \Rightarrow {}^3A_{2g}(F)$ and $^1T_{2g}(D) \Rightarrow {}^3T_{2g}(F)$ electronic transitions. However, in the last few years new emissions from the $^1T_{2g}(D)$ level have been observed in several chlorides [11], MgO [12] and different fluorides [9, 10].

In a recent paper we have presented the optical absorption, photoluminescence and lifetime measurements of Ni^{2+} in $RbCaF_3$ and $RbCdF_3$ [13] where only the three usual emissions were reported. In this work we present new results that include the $^1T_{2g}(D) \Rightarrow {}^3T_{1g}(F)$ emission as well as a detailed study of the low-temperature structure of the three emission bands coming from the $^1T_{2g}(D)$ level. The emission

0953-8984/93/060747+10$07.50

corresponding to the $^3T_{2g}(F) \Rightarrow {}^3A_{2g}(F)$ transition was too weak to obtain a resolved structure with our experimental set-up.

On the other hand it is well known that the structural phase transitions that appear in both $RbCaF_3$ and $RbCdF_3$ can induce changes in the spectroscopic properties of impurity ions [14–17]. Spectroscopic measurements of these impurities have been used to probe the transitions and give information about the local distortions. This type of study has been reported recently in $RbCdF_3$ [18] using Ni^{2+} as a probe. Ni^{2+} EPR spectra are sensitive to the cubic–tetragonal structural phase transition and provide some information about the thermal evolution of the order parameter. On the other hand no influence of the phase transition has been detected in the optical spectra.

A similar study is presented now for Ni-doped $RbCaF_3$. The EPR spectrum of Ni^{2+} ions in $RbCaF_3$ has been measured at different temperatures and the results interpreted taking into account a strain broadening of the signals as well as the influence of the cubic–tetragonal phase transition. The evolution of the order parameter for temperatures close to that of the transition (195 K) has been derived and a value of 0.24 has been obtained for the critical exponent in good agreement with values obtained using other experimental techniques [19, 20].

2. Experimental details

Single crystals of $RbCaF_3$ and $RbCdF_3$ containing Ni were grown by the Bridgman technique. The Ni content in the starting materials ranged from 0.5 to 2%. Absorption spectra were obtained on a Hitachi U-3400 spectrophotometer. The luminescence was excited with either a 150 W arc Xe lamp passed through a 0.25 m Bausch & Lomb monochromator or the 457.9 nm line of a 20 W CW Coherent Ar laser (Innova 200) and detected in the 300–850 nm ($\sim$ 33 000–12 000 cm^{-1}) region with a Hamamatsu R-928 photomultiplier placed at the exit slit of a 0.5 m Jarrel-Ash monochromator. A silicon avalanche photodiode C30955E from RCA was used to measure infrared emissions in the 1000–1100 nm (10 000–9000 cm^{-1}) region. Lines from a mercury lamp were used as wavelength references. Variable temperature measurements (10–300 K) were performed with a CTi Cryogenics close cycle cryo-refrigerator with a temperature stability better than ± 0.5 K.

EPR spectra were measured with a Varian E-112 spectrometer working in the X-band. For measurements at different temperatures a continuous flow helium cryostat (ESR900) from Oxford Instruments was used. Magnetic field values were determined with an NMR Gaussmeter, model ER035 from Bruker. The diphenylpicrylhydrazyl (DPPH) resonance signal ($g = 2.0037 \pm 0.0002$) was used as a standard to determine the microwave frequency.

3. Experimental results

The optical absorption spectra of both $RbCaF_3$:Ni and $RbCdF_3$:Ni crystals show three main bands centred at about 440, 880 and 1500 nm (22 500, 11 400 and 6700 cm^{-1}), a small one at about 670 nm (15 000 cm^{-1}) and a shoulder near 500 nm (20 000 cm^{-1}) which are due to the electronic transitions from the $^3A_{2g}(F)$ ground state to the $^3T_{1g}(P)$, $^3T_{1g}(F)$, $^3T_{2g}(F)$, $^1E_g(D)$ and $^1T_{2g}(D)$ levels respectively. This absorption spectrum has been measured at different temperatures from 300 K to 10 K and particularly at those close to the cubic–tetragonal phase transition (195 K in $RbCaF_3$

and 124 K in $RbCdF_3$) in order to see if we could detect the influence of the transition. Within our experimental accuracy no changes have been detected.

Several photoluminescence emissions can be observed in our crystals when we excite with light in the absorption bands. Exciting in the 22 500 cm^{-1} band we have detected three emissions at about 19 200, 13 500 and 9300 cm^{-1}. The first two have already been reported [13] and correspond to the transitions $^1T_{2g}(D) \Rightarrow {}^3A_{2g}(F)$ and $^1T_{2g}(D) \Rightarrow {}^3T_{2g}(F)$ while the third one, which has not been found before in these compounds, will be assigned to the $^1T_{2g}(D) \Rightarrow {}^3T_{1g}(F)$ electronic transition. In order to make this assignment we have measured the decay of the luminescence after switching off the excitation. This decay is exponential in samples with a low Ni^{2+} content and with the same decay time (780 μs and 490 μs for the Ca and Cd compounds respectively when measured at 10 K) when the detection is performed in any of the three emissions. This indicates that the three electronic transitions associated with these bands have the same initial level which has been previously identified as the $^1T_{2g}(D)$ [4, 5].

As in the case of the absorption spectrum we have performed our photoluminescence measurements at different temperatures but again we have not detected any influence that could be assigned to the structural phase transitions.

When measured at 10 K, a structure is observed in the three main emission bands as shown in figure 1. As discussed below most of the lines that are observed have a vibronic origin and correspond to transitions from the $^1T_{2g}(D)$ state to different levels of the final states. The structures of each of the bands are similar in both matrices. To stress this similarity the horizontal axes for Ca and Cd compounds have been shifted in the figure. The peak positions are given in table 1.

The EPR spectrum of Ni^{2+} in $RbCaF_3$ has been measured as a function of temperature (the results for $RbCdF_3$ were previously reported [18]). At temperatures above the phase transition an isotropic spectrum consisting of three lines is found (see figure 2(*a*)). The most intense one is a broad line (peak to peak width of about 80 mT) at $g = 2.36$ which will be called the normal line (NL). Superimposed on it and centred at the same g-value a narrower line is observed with the phase inverted which will be called the inverted line (IL). Finally another line, the half field line (HFL), appears at $g = 4.7$. This line is strongly asymmetric being more extended towards low fields.

At temperatures below T_c, $RbCaF_3$ crystals become tetragonal [14] and an anisotropic Ni^{2+} EPR spectrum is observed. In figure 2(*b*) the spectrum obtained at LNT with the magnetic field along one of the ⟨100⟩ directions is shown. Since we have a polydomain sample there are three different orientations for the tetragonal axis and we observe the lines corresponding to all of them. The positions of these lines change with the magnetic field orientation. A rotational diagram is given in figure 3. The width of the lines in the tetragonal phase is also a function of the angle Θ between the field and the tetragonal axis of the centres. The minimum width was obtained for $\Theta = 45°$.

Below the phase transition the positions of the EPR lines are strongly temperature dependent. They were measured as a function of temperature, with the magnetic field along a ⟨100⟩ direction. From these data we have obtained the spin Hamiltonian parameters at different temperatures. The evolution of the axial crystal field parameter (D) against T is given in figure 4 and from this evolution the critical exponent of the transition (β) has been derived (see below).

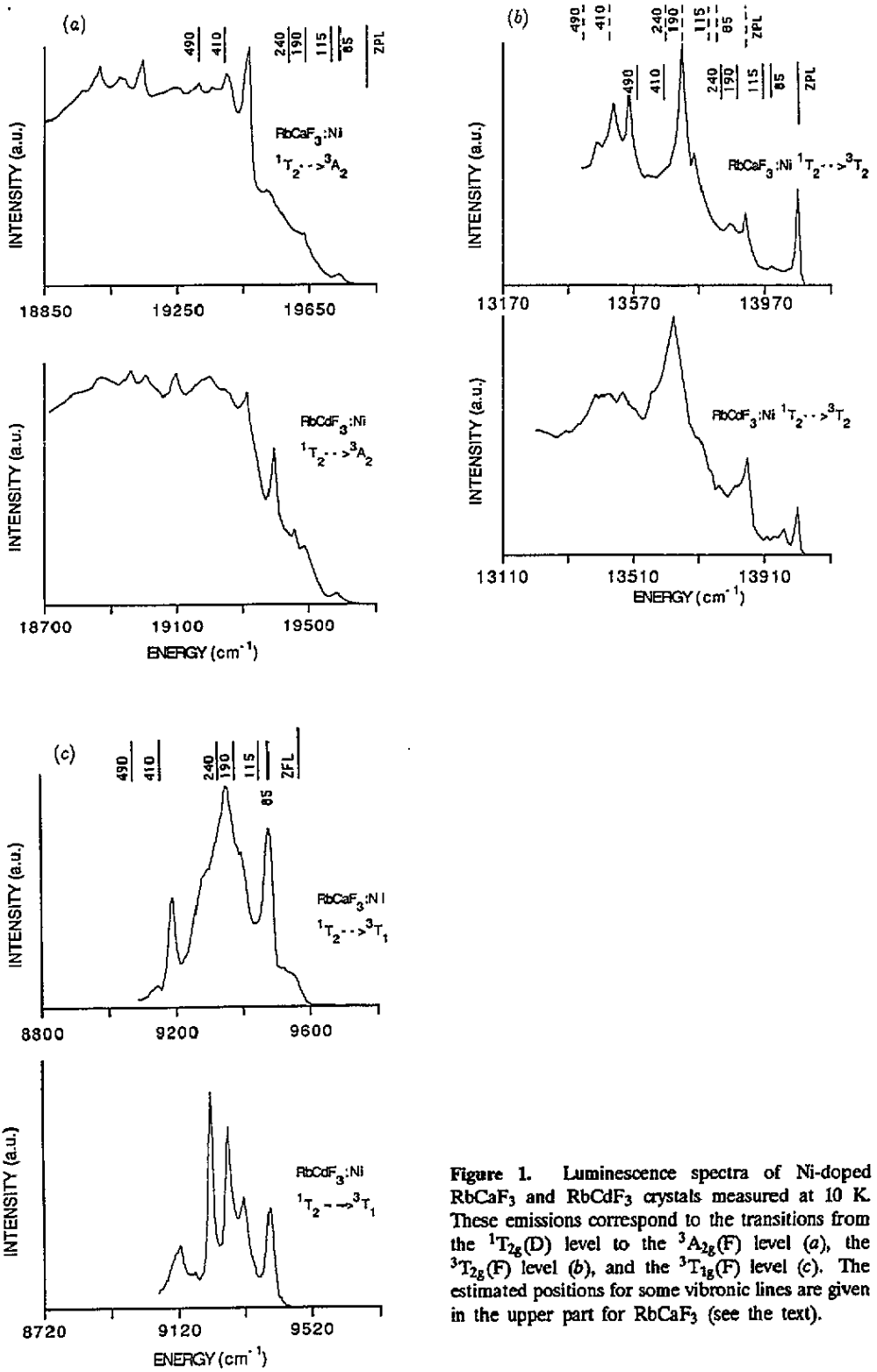

Figure 1. Luminescence spectra of Ni-doped $RbCaF_3$ and $RbCdF_3$ crystals measured at 10 K. These emissions correspond to the transitions from the $^1T_{2g}(D)$ level to the $^3A_{2g}(F)$ level (*a*), the $^3T_{2g}(F)$ level (*b*), and the $^3T_{1g}(F)$ level (*c*). The estimated positions for some vibronic lines are given in the upper part for $RbCaF_3$ (see the text).

Table 1. Emission line positions of $RbCaF_3$:Ni and $RbCdF_3$:Ni and energies of the odd phonon modes in $RbCaF_3$:Ni (in cm^{-1}).

	$^1T_{2g} \rightarrow {}^3A_{2g}$	$^1T_{2g} \rightarrow {}^3T_{2g}$	$^1T_{2g} \rightarrow {}^3T_{1g}$	Energies of odd modes
$RbCaF_3$:Ni	19741	14070	9556	85 (TO_1)
	19624	13913	9524	115 (LO_1)
	19526	13865	9482	190 (TO_2)
	19473	13755	9398	240 (LO_2)
	19408	13710	9352	410 (TO_3)
	19370	13632	9285	490 (LO_3)
	19325	13555	9188	184 (O_4)
	19242	13510		
	19144			
	19091			
	19020			
	18827			
	18704			
$RbCdF_3$:Ni	19588	14007	9392	
	19492	13963	9328	
	19458	13940	9266	
	19405	13856	9213	
	19315	13826	9162	
	19255	13714	9120	
	19207	13632		
	19164	13576		
	19095	13522		
	19000	13443		
	18953			
	18873			

4. Discussion

The optical absorption spectrum of Ni ions in the two compounds is easily understood as being due to Ni^{2+} in an octahedral environment with the crystal field and Racah parameters given in [13]. The lack of observable changes when we go through the cubic–tetragonal phase transition can be explained by the small changes of the Ni^{2+} environment.

In the case of the photoluminescence obtained by excitation in the 22500 cm^{-1} band, the new emission at 9300 cm^{-1} that we have detected besides the known ones at about 19200 cm^{-1} ($^1T_{2g}(D) \Rightarrow {}^3A_{2g}(F)$) and 13500 cm^{-1} ($^1T_{2g}(D) \Rightarrow {}^3T_{2g}(F)$) can be associated with the $^1T_{2g}(D) \Rightarrow {}^3T_{1g}(F)$ transition. Some recent papers have reported the observation of this emission in several ionic crystals, in particular $KMgF_3$ and $KZnF_3$ [10]. Our assignment is based on the same lifetime value obtained for the decay of this emission as for the other two that come from the $^1T_{2g}(D)$. This is an indication that the three emission bands have the same initial level. On the other hand the transition that goes to the $^1E_g(D)$ should appear at energies lower than 9300 cm^{-1} as can be easily seen from the positions of the energy levels obtained from the optical absorption spectra. From all this we conclude the proposed assignment for the new emission. It is worth mentioning that the low intensity of the 9300 cm^{-1} emission and the low efficiency of the infrared detectors may explain why this emission has not been detected previously. We have used an Si avalanche photodiode which sensitivity is good at 10000 cm^{-1} but decreases very sharply at lower energies. Because of this

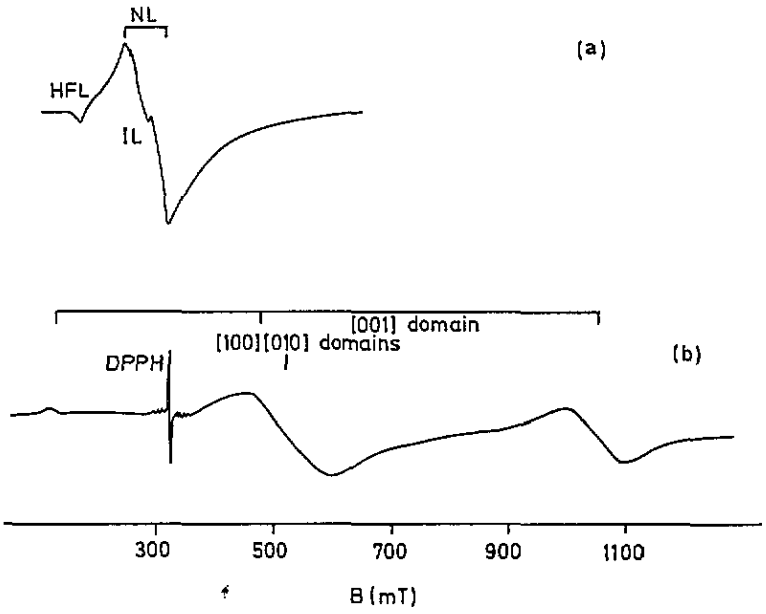

Figure 2. EPR spectra of Ni^{2+} ions in $RbCaF_3$: (*a*) measured in the cubic phase and (*b*) measured at 77 K in a polydomain sample with the magnetic field along a pseudocubic ⟨100⟩ direction. The signal at about 320 mT is due to traces of Mn^{2+} impurities.

we have not corrected the emission band for the instrument response and it is likely that its shape is distorted, mainly in the low-energy region (see below).

With respect to the band associated with the $^1T_{2g}(D) \Rightarrow {}^1E_g(D)$ transition we must say that it should appear at energies lower than those detectable with our Si photodiode. We have tried to find it using other infrared detectors but we have not succeeded. This emission has not been reported either in $KMgF_3$ or in $KZnF_3$ and in some of the other cases where it has been observed its intensity was much lower than that of the $^1T_{2g}(D) \Rightarrow {}^3T_{1g}(F)$ transition in spite of the latter being spin forbidden and the former spin allowed. This behaviour has been discussed by several authors [11, 12].

The analysis of the structure observed in the different emission bands is complicated because in some cases we cannot easily determine the purely electronic origin (zero phonon line: ZPL) of the emissions and in some others there are several spin–orbit (SO) components in the final state. Besides, at temperatures of 10 K the point symmetry around the divalent cation position is not the O_h corresponding to 300 K but D_{2h} in $RbCaF_3$ [21] and D_{4h} in $RbCdF_3$ [22] and this could produce an extra splitting of the electronic levels. However, since our results are similar to those already published for Ni^{2+} in other fluoroperovskites that do not present phase transitions [4, 10] we conclude that, in agreement with the optical measurements that we have performed at temperatures close to those of the transition, no clear influence of the phase transitions on the low-temperature structure of the luminescence emissions has been observed in our crystals. On the other hand, it is worth mentioning that although the bands corresponding to the two compounds are similar, the structure looks very different in the three emission bands.

Beginning with the $^1T_{2g}(D) \Rightarrow {}^3T_{1g}(F)$ band the observed structure is similar, except

for some small bands that appear in the high-energy side in $RbCaF_3$, to the one given in [10] associated with the transition from the emitting level to the Γ_4 SO component of the $^3T_{1g}(F)$. Assuming this assignment we have calculated the positions of the other SO components of the $^3T_{1g}(F)$ level using the matrices given by Liehr and Ballhausen [23], the approximate crystal field and Racah parameters derived from a crystal field analysis of the optical absorption spectra and an SO coupling constant $\lambda = 300\ cm^{-1}$ (see below). We have found that the transition to the Γ_3 and Γ_5 components of the $^3T_{1g}(F)$ level that have been observed in the spectra given in [10] would be outside the detection range of our Si detector while the magnetic dipole (MD) transition to the Γ_1 component that will appear in the high-energy side of our spectrum is forbidden.

Following [10] we have tried to assign the observed structure to vibronic transitions associated with interactions with odd phonon modes. The low intensity of the MD allowed transition to the Γ_4 level, barely visible in [10] and undetectable in our crystals, together with the lack of equally spaced series of replicas in our spectra indicate that the structure is not due to interactions with even phonon modes. With respect to the odd modes only in the case of $RbCaF_3$ we have been able to find in the literature some information about their frequencies at $k = 0$ (measured at temperatures down to 100 K) [24]. Their values and mode assignments are given in table 1. Taking the first intense peak in the structure of both compounds as due to the interaction with the lowest-energy phonon we have plotted in figure 1(*c*) the positions of the lines that could appear in the spectrum of $RbCaF_3$:Ni due to interactions with one phonon of each of the odd modes. The agreement between the predicted line positions and the observed ones is reasonable.

Concerning the structure of the $^1T_{2g}(D) \Rightarrow {}^3T_{2g}(F)$ transition (figure 1(*b*)) we should take into account the SO splitting of the final level. The line at the highest energy is narrower than most of the others and it has been assigned in similar compounds to the ZPL of the MD allowed transition from the emitting level to the lowest of the SO components (Γ_3) of the $^3T_{2g}(F)$ level. The positions calculated for the transitions to the other SO components of the $^3T_{2g}(F)$ state have been estimated as in the case of the $^3T_{1g}(F)$ level. These positions are shifted approximately 150 cm^{-1} (Γ_4), 540 cm^{-1} (Γ_5) and 680 cm^{-1} (Γ_2) towards the low-energy side. A narrow line at about 150 cm^{-1} observed in the spectra of both compounds can be assigned to the transition to the Γ_4 component while the electronic origins corresponding to the other SO levels are not distinguished in our spectra.

The rest of the structure could be due to replicas of the ZPL corresponding to interactions with even phonon modes. However, this should give progressions of lines that are not clear in our measurements. The other possibility for the structure is to have electric dipole (ED) allowed transitions due to interaction with odd phonon modes. As in the case of the $^1T_{2g}(D) \Rightarrow {}^3T_{1g}(F)$ transition we have plotted in figure 1(*b*) the estimated positions of the vibronic lines associated with interactions with the odd $k = 0$ vibrations for $RbCaF_3$. Electronic origins have been taken in the two ZPLs that we have previously discussed. Again a reasonable agreement between predicted and observed line positions is obtained.

With respect to the 19 200 cm^{-1} band, no electronic origin is observed and we have not found any hot transition as in other cases reported in the literature [4]. The lines should be associated with vibronic lines that are ED allowed through interaction with odd phonon modes and with replicas involving both odd and even modes. Assuming that the first line is due to the interaction with the odd mode of lowest energy we give

in figure 1(*a*) the positions estimated for the other lines in $RbCaF_3$ corresponding to one phonon of each of the odd parity modes. The agreement with the observed spectrum is poor and it does not improve if the first line is associated with other odd phonons at higher energies. In particular, it seems that the main line in the spectrum can hardly be associated with any of the vibronic transitions due to interactions with odd phonons of the lattice at $k = 0$. It seems that in our crystals the structure of the three observed bands cannot be explained taking into account the interactions with the same phonon modes, in contrast with the results obtained by other authors [4, 25, 26]. On the other hand, there are some cases where the fine structure of the absorption and emission bands of Ni^{2+} impurities cannot be explained without taking into account a dynamic Jahn–Teller (JT) effect [27, 28]. We think that this JT coupling should be considered to give an appropriate description of the fine structure of our bands. However, since we cannot make a precise determination of the electronic origins of the 19 200 cm^{-1} and 9300 cm^{-1} bands and because of the scarce information presently available on the phonon structures of the pure $RbCaF_3$ and $RbCdF_3$ compounds at low temperatures (10 K), it is difficult to draw more reliable conclusions from our results.

We will discuss now the EPR spectra of Ni^{2+} in $RbCaF_3$ at different temperatures. Above the phase transition (195 K) the spectrum corresponds to Ni^{2+} ions in a cubic octahedral environment. When the static magnetic field $\boldsymbol{B}$ is applied the $S = 1$ ground state ($^3A_{2g}(F)$) is split in the $|0\rangle$ and $|\pm 1\rangle$ spin levels and an isotropic line (NL) should be observed due to the $|0\rangle \Leftrightarrow |\pm 1\rangle$ EPR allowed transitions. Due to residual strains a distribution of the levels splittings is produced and consequently a broadening of the line as reported in many cases [29–31]. The line position can be described using the spin Hamiltonian

$$H = g\mu_B \boldsymbol{S} \cdot \boldsymbol{B} \tag{1}$$

with $S = 1$ and an isotropic g-factor of $g = 2.36 \pm 0.01$.

From the ligand field theory this g-factor is given, up to first order, by

$$g = g_e - (8\lambda/\Delta) \tag{2}$$

where λ is the effective SO coupling constant, g_e the free electron g-factor and $\Delta = 10$ Dq, which in our case corresponds to the energy difference between the ground state $^3A_{2g}(F)$ and the first excited state $^3T_{2g}(F)$. Using the values of Δ obtained from our optical absorption spectrum and the measured g-factor we found $\lambda = -300$ cm^{-1} which is in good agreement with values reported for Ni^{2+} in similar compounds [1, 18] and corresponds to a reduction of about 10% with respect to the free ion value.

The IL that appears at the same position as the NL has been associated by Smith *et al* [30] with the changes introduced in the shape of the NL absorption due to the broadening of the absorption lines of sites with strain-induced shifts smaller than the homogeneous linewidth of the EPR line. That broadening is due to cross-relaxation between the $|+1\rangle \Leftrightarrow |0\rangle$ and $|-1\rangle \Leftrightarrow |0\rangle$ transitions.

Finally the line that appears at $g \simeq 4.7$ (HFL) corresponds to the forbidden transition $|+1\rangle \Leftrightarrow |-1\rangle$, which in our case becomes partly allowed because of the mixing among Zeeman states produced by the strain–spin coupling. The asymmetry of the line with a tail towards low fields can be understood taking into account the relationship between the line position and the transition probability [32].

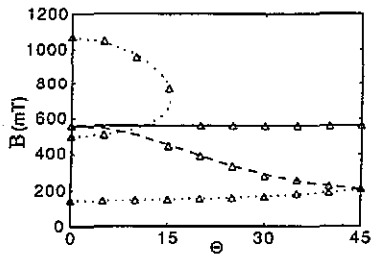

Figure 3. Rotational diagram of Ni^{2+} ions in the tetragonal phase. The observed positions of the EPR lines measured at 77 K in a polydomain sample are represented by triangles (△). The curves represent the theoretical evolution, calculated using the spin Hamiltonian (3) and the values given in the text. The different traces correspond to domains in the three different directions. The angle Θ is measured from the pseudocubic [001] direction.

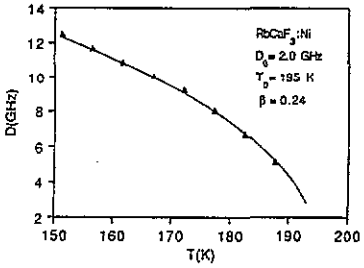

Figure 4. Evolution of the crystal field parameter D against T for tetragonal Ni^{2+} ions in $RbCaF_3$. The experimental values are represented by full triangles (▲). The continuous line corresponds to the evolution predicted by equation (4) with the parameters given in the figure.

At temperatures below the phase transition the crystal becomes tetragonal. The fluorine octahedra surrounding the divalent cations are elongated in one of the ⟨100⟩ directions and rotate by an angle Φ around this direction, the rotation being alternated in neighbouring octahedra. The tetragonal distortion and the angle Φ are temperature dependent. Different domains oriented along each of the ⟨100⟩ directions are usually observed. The line positions given in figure 3 correspond to the three different orientations of the Ni^{2+} tetragonal axis. Taking this into account a fitting can be performed with the positions obtained using the following spin Hamiltonian:

$$H = \mu_B \boldsymbol{B}(g_\perp \sin\Theta S_x + g_\parallel \cos\Theta S_z) + D\left[S_z^2 - (1/3)S(S+1)\right] \quad (3)$$

with $S = 1$. The z axis is along the tetragonal axis of each of the centres and Θ is the angle between the z axis and the direction of the applied static magnetic field $\boldsymbol{B}$. The best fit between the positions calculated using this spin Hamiltonian and the observed positions is given in figure 3. The corresponding spin Hamiltonian parameters are $g_\parallel = 2.32 \pm 0.01$, $g_\perp = 2.30 \pm 0.01$ and $D = 25.3 \pm 0.5$ GHz.

The lines in the tetragonal phase are as broad as the NL in the cubic phase and the minimum width is obtained for Θ close to 45°. HFL is also observed when the magnetic field is applied along the tetragonal axes. As explained in [18] all this indicates that the strain–spin coupling is still strong in the tetragonal phase.

Finally we will discuss the thermal evolution of the crystal field parameter D. The values of D measured at different temperatures, not far from that of the phase transition, are presented in figure 4 and can be fitted to the expression

$$D(T) = D_0|T - T_0|^{2\beta} \quad (4)$$

with $D_0 = 2.0$ GHz, $T_0 = 195$ K and $\beta = 0.24$.

This behaviour corresponds to the following. The crystal field parameter D has a quadratic dependence on the tilting angle of the fluorine octahedra Φ which is the order parameter in the 195 K structural phase transition of $RbCaF_3$ [33]. On the other hand the temperature dependence of the order parameter at temperatures not far from T_0 is given by [34]. $\Phi(T) = \Phi_0|T - T_0|^\beta$ where β is the critical exponent.

The value of $\beta = 0.24$, that we have obtained, is close to the one previously found in $RbCdF_3$ [18] and is in agreement with the results derived using other experimental techniques [19–21]. Thus we conclude that as in the case of $RbCdF_3$ the EPR spectra of Ni^{2+} ions can be used as a probe to obtain information about the structural phase transition in $RbCaF_3$ and in particular to find the value of the critical exponent β.

Acknowledgments

We wish to thank Dr F Rodríguez and Dr M Moreno (Universidad de Cantabria, Santander, Spain) for helpful discussions. This work was sponsored by the Spanish DGICYT under contract number PB90-0918.

References

[1] Ferguson J, Guggenheim H J and Wood D L 1964 *J. Chem. Phys.* **40** 822
[2] Hush M S and Hobbs R J M 1968 *Progress in Inorganic Chemistry* vol 10, ed F A Cotton (New York: Interscience) p 259
[3] Ferguson J 1970 *Progress in Inorganic Chemistry* vol 12, ed S J Lippard (New York: Interscience) p 159
[4] Veshe W E, Lee K H, Yun S J and Sibley W A 1975 *J. Lumin.* **10** 149
[5] Iverson M V and Sibley W A 1979 *J. Lumin.* **20** 311
[6] Johnson L F, Dietz R E and Guggenheim H J 1963 *Phys. Rev. Lett.* **11** 318
[7] Johnson L F, Guggenheim H J, Bahnck D and Johnson A M 1983 *Opt. Lett.* **8** 371
[8] Moncorgé R and Benyattou T 1988 *Phys. Rev.* B **37** 9186
[9] Tonuvi R J, Jacobsen S M and Yen W M 1990 *J. Lumin.* **46** 155
[10] May P S and Güdel H U 1990 *Chem. Phys. Lett.* **175** 488
[11] May P S and Güdel H U 1989 *Chem. Phys. Lett.* **164** 612
[12] Payne S A 1990 *Phys. Rev.* B **41** 6109
[13] Alcalá R, Casas-González J, Villacampa B and Alonso P J 1991 *J. Lumin.* **48&49** 569
[14] Mo[illegible]e F A, Sonder E, Unruch W P, Finch L B and Westbrook R D 1974 *Phys. Rev.* B **10** 1623
[15] Rousseau J J, Rousseau M and Fayet J C 1976 *Phys. Status Solidi* b **73** 625
[16] Arakawa M 1979 *J. Phys. Soc. Japan* **46** 1245
[17] Studzinski P and Spaeth J M 1986 *Phys. Status Solidi* b **136** 735
[18] Alcalá R, Alonso P J and Spaeth J M 1990 *Phys. Rev.* B **41** 10 902
[19] Jex M, Maetz J and Müllner M 1980 *Phys. Rev.* B **21** 1209
[20] Maetz J, Müllner M, Jex H and Peters R 1980 *Solid State Commun.* **18** 1239
[21] Bulou A, Ridou C, Rousseau M, Nouet J and Hewat A W 1980 *J. Physique* **41** 87
[22] Rousseau M, Gesland J Y, Juilfard J, Nouet J, Zarembowitch J and Zarembowitch A 1975 *Phys. Rev.* B **12** 1579
[23] Liehr A D and Ballhausen C J 1959 *Ann. Phys., NY* **2** 134
[24] Ridou C, Rousseau M and Gervais F 1986 *J. Phys. C: Solid State Phys.* **19** 5757
[25] Sturge M D 1971 *Solid State Commun.* **9** 899
[26] Rodríguez F, Riesen H and Güdel H U 1991 *J. Lumin.* **50** 101
[27] Kaufmann U, Koidl P and Schirner O F 1973 *J. Phys. C: Solid State Phys.* **6** 310
[28] Kaufmann U G and Koidl P 1974 *J. Phys. C: Solid State Phys.* **7** 791
[29] Stoneham A M 1966 *Proc. Phys. Soc.* **89** 909
[30] Smith S R P, Dravnieks F and Wertz J E 1969 *Phys. Rev.* B **178** 471
[31] Bowden C M, Meyer H C and Donoho P L 1971 *Phys. Rev.* B **3** 645
[32] McMahon D H 1964 *Phys. Rev.* A **134** 28
[33] Owen F J 1979 *Magnetic Resonance of Phase Transitions* ed F J Owen *et al* (New York: Academic) ch 6
[34] Lines M E and Glass A M 1979 *Principles and Applications of Ferroelectric and Related Materials* 1st edn (Oxford: Clarendon)